



Cite this: RSC Adv., 2022, 12, 17264

# Physicochemical properties, immunostimulatory and antioxidant activities of a novel polysaccharide isolated from *Mirabilis himalaica* (Edgew) Heim

Surina Bo,<sup>a</sup> Mu Dan,<sup>a</sup> Wenjie Han,<sup>a</sup> Sarangua Ochir,<sup>\*b</sup> Liang Bao,<sup>b</sup> Lingwei Liu,<sup>b</sup> Tegshi Muschin<sup>\*c</sup> and Huricha Baigude<sup>\*d</sup>

Herbal medicines often contain bioactive polysaccharides. However, many medicinal herbs have not been explored for any active saccharides that may play key roles in their bioactivities. Herein, we extracted a novel polysaccharide from *Mirabilis himalaica* (Edgew) heim (denoted MHHP), a popular medicinal ingredient in traditional medicines. The structural and morphological characteristics of MHHP were measured and elucidated by high-performance gel permeation chromatography, gas chromatography connected with mass spectrometry, Fourier transform infrared and nuclear magnetic resonance spectroscopy as well as scanning electron microscopy. MHHP was homogeneous with a molecular weight of 16.1 kDa,  $M_w/M_n = 1.33$ , containing mainly  $\alpha$ -D-glucan residues with (1→4)-linkage. The biological activities of MHHP upon proliferation of splenic lymphocyte, activation of related cytokine and production of nitric oxide (NO) in RAW264.7 cells were investigated *in vitro*. MHHP induced proliferation of mouse spleen lymphocytes and significantly promoted the secretion in TNF- $\alpha$ , IL-6 and NO production in RAW264.7 cells. Meanwhile, MHHP exhibited relatively low antioxidant abilities. Our data suggested that MHHP may have potential immunoregulatory and anti-inflammatory activity, with a moderate antioxidant activity.

Received 11th January 2022

Accepted 17th May 2022

DOI: 10.1039/d2ra00060a

rsc.li/rsc-advances

## 1. Introduction

Nyctaginaceae (*Mirabilis*) is a sod-forming perennial plant which is mainly found in tropical regions. There are about 60 species in the world and 3 are found in China, including *Mirabilis jalapa*, *Mirabilis var chinesis* Heimerl and *Mirabilis himalaica*. *Mirabilis himalaica* is a well-applied herbal plant species that grows on the high mountains of the Tibet Plateau.<sup>1</sup> The tap roots of *M. himalaica* plants have been widely used for various disease treatments, such as nephritic edema, gonorrhea, and stomach disorders by Tibetan and Mongolian people for more than 1000 years.<sup>2–4</sup> According to Mongolian medicine theory, *Mirabilis himalaica* (Edgew) heim is one of the four traditional root tonic Mongolian medicines, which also includes *Asparagus cochinchinensis* (lour) merr, *Polygonatum odoratum* (Mill.) Druce, and *polygonatum sibiricum* Delar ex redoute. *M. himalaica* has

widely been used to treat many diseases, including kidney warming, kidney nourishment, tissue regeneration, urination, and urinary calculus removal effects.<sup>5,6</sup>

However, there is very little literature on the natural compounds and related biological activities of *Mirabilis himalaica*. Chemical analysis of *Mirabilis himalaica* was restricted to several compounds including amides, glycolipids, and sterol-oleandoleic acid.<sup>7,8</sup> The typical bioactive compound of *M. himalaica* is the retinoid that is reported to exhibit anti-tumor activity.<sup>9</sup> Another chemical investigation of biological activity on mirabijalone E isolated from *M. himalaica* was carried out *in vitro* and *in vivo*. Mirabijalone E inhibited growth of non-small cell lung cancer cells (A549 cells) in a time and dose-dependent manner.<sup>10</sup>

The chemical composition in root herbs vary in complexity and diversity, of which polysaccharides form an important effective chemical component. Modern pharmacological studies have shown that most polysaccharides isolated from more than 30 species of root herbs have multiple biological effects such as anti-infection,<sup>11,12</sup> anti-diabetic activity,<sup>13,14</sup> anti-tumor,<sup>15,16</sup> antioxidant,<sup>17,18</sup> immunomodulation,<sup>19,20</sup> anti-inflammation,<sup>21,22</sup> anti-viral,<sup>23</sup> delaying aging<sup>24</sup> and hypoglycemia.<sup>25</sup> Many Chinese tonic medicines with complementary effects contain polysaccharides to regulate the body's immune functions, such as promoting immune cell proliferation and differentiation, activation of immune cells, secretion of immunomodulating related cytokines and so on.<sup>26,27</sup>

<sup>a</sup>College of Pharmacy, Inner Mongolia Medical University, Jinshan Development Zone, Hohhot, Inner Mongolia, 010110, P. R. China

<sup>b</sup>Academy of Mongolian Medicine, Inner Mongolia Medical University, Jinshan Development Zone, Hohhot, Inner Mongolia, 010110, P. R. China. E-mail: 3275932783@163.com; Tel: +86-0471-6653165

<sup>c</sup>Inner Mongolia Key Laboratory of Green Catalysis, College of Chemistry and Environmental Science, Inner Mongolia Normal University, Inner Mongolia, 010022, P. R. China. E-mail: tegshimsch@163.com; Tel: +86-0471-6990751

<sup>d</sup>Institute of Mongolian Medicinal Chemistry, School of Chemistry & Chemical Engineering, Inner Mongolia University, Hohhot, Inner Mongolia, 010020, P. R. China. E-mail: hbaigude@imu.edu.cn; Fax: +86 471 4992511; Tel: +86 471 4992511



In the immune system, activation of immune cells such as macrophages, lymphocytes, and dendritic cells play an essential role in enhancing immunity.<sup>28,29</sup> Polysaccharides isolated from traditional Mongolian herbs have been shown to stimulate the innate immunity and cellular immunity by interacting with immune cells,<sup>30,31</sup> regulate the immune response in an appropriate way, and promote the body's immune system to resist bacterial or viral infections.

In order to further explore the chemical structure of polysaccharides isolated from *Mirabilis himalaica* with potential biological activities *in vitro*, in this work, we prepared homogeneous molecular weight polysaccharide and characterized structurally and morphologically through Fourier transform infrared spectroscopy (FT-IR), high performance anion-exchange chromatography coupled with pulsed amperometric detection (HPAEC-PAD), nuclear magnetic resonance (NMR), scanning electron microscopy (SEM), high performance gel permeation chromatography (HPGPC) and methylation analysis. Its immunostimulatory activity was evaluated by mouse spleen lymphocytes and macrophages RAW 264.7 cell assay *in vitro* as well, and the *in vitro* antioxidant activity was estimated by three radical scavenging methods. Therefore, this work aims to provide fundamental information of the structure characterization, immunostimulatory and antioxidant activities of polysaccharide purified from *Mirabilis himalaica*.

## 2 Material and methods

### 2.1 Chemical and materials

Roots of *Mirabilis himalaica* (Edgew) heim were purchased from Qinghai Tibetan hospital in Qinghai (batch number: 20161023; Xining, Qinghai province, China). Dextran standards (5800, 11 800, 47 300, 100 000, 380 000, and 788 000 Da) were acquired from Pharmacia Biotech (Uppsala, Sweden). Standard monosaccharides (glucose, D-glucosamine hydrochloride, mannose, rhamnose, ribose, galactose, fucose, N-acetyl-D-glucosamine, D-galactosamine hydrochloride, xylose, fructose, arabinose, guluronic acid, mannuronic acid, galacturonic acid, glucuronic acid) were purchased from Sigma chemical. Dialysis membranes (size 36, MW<sub>CO</sub> = 8–14 kDa) were purchased from Wako. Acetic acid, acetic anhydride, sodium borohydride, chloroform, NaOH powder, DMSO, iodomethane, formic acid, methanol, trifluoroacetic acid were all analytical reagents.

### 2.2 Isolation, purification and molecular weight of the polysaccharides

Crude MHHP was refluxed and extracted three times in a 85 °C water bath by heating for 1 h and filtered with gauze. The filtrates that combined and concentrated to a certain volume were precipitated up to 80% ethanol concentration and kept overnight. The precipitate was obtained by centrifugation (8000 rpm, 12 min, 4 °C), then washed three times with anhydrous ethanol and acetone for decolorization, then the precipitate was vacuum dried at 50 °C to achieve the water-soluble crude sample of *Mirabilis himalaica* (Edgew) heim. Crude MHHP polysaccharide was adopted to use the trypsin enzyme-

savage combination method to remove the proteins and loaded onto a pre-equilibrated DEAE Sepharose Fast Flow chromatography column (2.6 × 100 cm) at a flow rate of 2.5 mL min<sup>-1</sup>, followed by an elution step with distilled water, 0.1 M, 0.2 M NaCl solution. The one mainly eluent fraction namely MHHP was collected and concentrated at 50 °C with a rotary vacuum evaporator, and then dialyzed (size 36, MWCO > 8.000 Da) with ultrapure water for 48 h, and freeze-dried. The sugar content of MHHP was measured by the phenol sulfuric acid method using UV-Vis spectrometer at 490 nm.<sup>32,33</sup> The content of protein was determined by BCA protein assay kit (Solarbio, China) using Microplate reader at 562 nm. Determination of the average-molecular weight of the MHHP was performed by high performance gel permeation chromatography (HPGPC) according to the previous mentioned method.<sup>34</sup> The calibration curve was plotted by Dextran standards with different molecular weights.

### 2.3 Monosaccharide composition

Chromatography was performed by a GC-MS QP2010 GC system (Shimadzu) equipped with an RXI-5 SIL MS column (30 m × 0.25 mm, 250 μm) (Agilent 19091J-413) under the following conditions: starting at a temperature 120 °C, then raised to 250 °C at a rate of 3 °C min<sup>-1</sup> and held for 5 min. The injector and detector temperatures were both set at 250 °C. The flow rates of H<sub>2</sub> and air were 30 mL min<sup>-1</sup> and 400 mL min<sup>-1</sup>, respectively. The carrier gas was He, and the flow rate was up to 1.0 mL min<sup>-1</sup>. GC analysis was employed to detect the monosaccharide composition of MHHP.

A MHHP sample (2 mg) was hydrolyzed in trifluoroacetic acid (TFA) (2 M, 1 mL) at 120 °C for 90 min. The hydrolysate was repeatedly concentrated with methanol (2 mL) until dried and reduced by adding double-distilled water (2 mL) and sodium borohydride (100 mg) at room temperature, then neutralized by acetic acid. The reduzate was repeatedly concentrated with methanol (3 mL) until dried again and acetylated by 1 mL acetic anhydride at 100 °C for 1 h. Then, the sample was cooled down and repeatedly concentrated with methylbenzene (3 mL) to remove excess anhydride. The acetylated derivative was dissolved in chloroform (3 mL), transferred into a separating funnel and shaken with distilled water 5 times. The chloroform layer was dehydrated by anhydrous sodium sulfate, and the final volume was increased to 10 mL for analysis.

### 2.4 UV absorption peak detection

A UV spectrophotometer (TU-1901, Persee, Beijing, China) was applied to scan a MHHP distilled water solution with a concentration of 1 mg mL<sup>-1</sup>, with scan range setting between 190 and 400 nm to detect wavelength range of 260 nm and 280 nm.

### 2.5 Infrared (IR) spectrum of the polysaccharide

FT-IR spectrum of the MHHP ground with KBr (1 : 100) was recorded on an IR Affinity Fourier transform infrared spectrometer (Shimadzu, Japan) with a resolution of 0.1 cm<sup>-1</sup> in the scanning range of 4000–400 cm<sup>-1</sup> using the KBr-disk method.<sup>35</sup>



## 2.6 Methylation analysis

Automatic reduction of carboxyl groups instrument (BR-HYY-001, utility model patent, no. 201921159550.2) was applied to uranic acid reduction of acidic polysaccharide MHHP. In detail, 80 mg MHHP was dissolved by distilled water, and then a uranic acid activator (*N*-(3-dimethylaminopropyl)-*N'*-ethylcarbodiimide hydrochloride) was added. The reduction instrument was set to pH 4.8 and reacted for 3 h and then at pH to 6.8 for 2 h. The samples were concentrated, dialyzed, and repeatedly reduced 3–5 times, and lyophilized. The resulting sample was subjected to methylation analysis.

The polysaccharide sample was dissolved in DMSO. Then NaOH powder was added quickly, sealed, and dissolved by ultrasound. And then methyl iodide was added for reaction. Finally, water was added to the above mixture to terminate the methylation reaction and the methylated polysaccharide continue to hydrolyze and acetylate as published method,<sup>36</sup> and analyzed by Shimadzu GCMS-QP 2010 gas chromatography-mass spectrometry to determine the sample of acetylated product.

GC-MS conditions as follows: RXI-5 SIL MS column (30 × 0.25 × 0.25), programmed temperature rising conditions are: initial temperature 120 °C, 3 °C min<sup>-1</sup> to 250 °C min<sup>-1</sup>; hold for 5 min; inlet temperature 250 °C, detector temperature 250 °C min<sup>-1</sup>, carrier gas is He with a flow rate of 1 mL min<sup>-1</sup>.

## 2.7 NMR spectroscopic analysis

35 mg of MHHP was dissolved in 600 μL D<sub>2</sub>O with 3-(trimethylsilyl)-1-propanesulfonic acid sodium salt (DSS) as an internal standard, then transfer to the NMR tube. The one- and two-dimensional <sup>1</sup>NMR, <sup>13</sup>C NMR spectra were recorded with a Bruker Avance III 500 NMR spectrometer (Bruker (Beijing) Scientific Technology Co., Ltd, Beijing, China) at 40 °C for 2 days.

## 2.8 Scanning electron microscope

The MHHP was coated with a thin layer of gold using a sputter coater, then the morphology of the polysaccharide was characterized on Hitachi S-4800 scanning electron microscopy (SEM) at 20 kV (Hitachi S-4800, Japan) at different magnifications with high vacuum conditions.

## 2.9 Immunomodulatory activity of MHHP

### 2.9.1 Activation effect of MHHP on mouse spleen lymphocytes

**2.9.1.1 Preparation of mouse spleen lymphocytes.** Approximately 7–8 week-old BALB/C male mice weighing 20 ± 2 g were obtained from the Laboratory Animal Center of Inner Mongolia Medical University. The preparation of spleen cell was processed using the above method.<sup>34</sup>

**2.9.1.2 Effect of MHHP on spleen lymphocyte proliferation.** 100 μL of the lymphocyte cell suspension (5 × 10<sup>6</sup> cells per mL) was seeded in a 96-well plate using RPMI 1640 medium. The plated cells were stimulated with RPMI 1640 alone as negative control, 2.5 μg mL<sup>-1</sup> of ConA as the positive control group, 200,

40 and 5 μg mL<sup>-1</sup> of MHHP as experiment groups; After 48 h of incubation (5% CO<sub>2</sub>, 37 °C), CKK-8 was pipetted to different groups, and each sample was measured at 450 nm using an ELISA micro plate reader (Thermo Electron Corporation, USA). Cell viability was calculated as the previous study.<sup>34</sup> Cell viability differences were compared using paired Student's *t*-test.

**2.9.1.3 Measurements of IFN-γ and IL-2.** The cell suspensions simulated by MHHP in different groups were obtained as described above. IFN-γ and IL-2 ELISA kits ((Dakewe Bio-engineering Co., Ltd, Shenzhen, China) were used to assess their cytokine levels according to the manufacture's protocol. The cytokine standard was serially diluted from 500 pg mL<sup>-1</sup> to 7.8 pg mL<sup>-1</sup> as the kit's manual advised.

### 2.9.2 Activation effect of MHHP on macrophage *in vitro*

**2.9.2.1 Secretion levels of TNF-α, IL-6 and IL-1β.** Cell culture was prepared as mentioned previous study.<sup>34</sup> RAW 264.7 cells were seeded in 96-well plates (1 × 10<sup>6</sup> cells per well) and were incubated with MHHP polysaccharide at different concentrations (5, 40 and 200 μg mL<sup>-1</sup>) for 48 h. The cells treated with the medium alone were used as blank control. The cells treated with 2.5 μg mL<sup>-1</sup> LPS (Melone-pharma, Daliang, China) were considered as a positive control. RAW 264.7 cells culture supernatant were harvested to quantify the level of IL-6, TNF-α and IL-1β, with the corresponding commercially available Mouse precoated Elisa kits (Dakewe Bio-engineering Co., Ltd, Shenzhen, China) according to the manufactures' instructions. The absorbance was measured at 450 nm with a microplate reader (Spectramax i3x, Molecular Devices, American).

**2.9.2.2 *In vitro* nitric oxide (NO) production assay.** 500 μL macrophage cell suspensions were plated into a 48-well plate at a concentration of 1 × 10<sup>5</sup> cells per mL using RPMI 1640. We applied 2.5 μg mL<sup>-1</sup> LPS in the 100 μL suspension in positive control group, and 5, 40, 200 μg mL<sup>-1</sup> polysaccharide in the experimental group, and the final volume of each well was 200 μL. After 48 h of incubation (5% CO<sub>2</sub>, 37 °C), the cell culture supernatant in each well were collected, and the NO content was measured by the Griess detection method according to the instructions of the NO kit. The absorbance was determined at 540 nm on a microplate reader and all analysis was performed in triplicate.

## 2.10 Antioxidant activity of MHHP

**2.10.1 DPPH radical scavenging activity assay.** The scavenging DPPH radical activity of the MHHP polysaccharide was evaluated according to the reported method.<sup>37</sup> Briefly, polysaccharide powder dissolved in distilled water reached the different concentrations (0.02–0.2 mg mL<sup>-1</sup>), then 2 mL of a freshly prepared DPPH ethanol solutions (1 × 10<sup>-5</sup> g mL<sup>-1</sup>) were mixed to same volume of the polysaccharide samples. The mixture was reacted at room temperature for 30 min in the dark, and the absorbance was measured at 517 nm. In this study, ascorbic acid (ASA) served as positive control. The scavenging activity was calculated with the following equation:

$$\text{Scavenging activity (\%)} = (1 - A_{\text{sample}}/A_{\text{control}}) \times 100\%$$



where  $A_{\text{control}}$  was the absorbance of DPPH solution without any sample,  $A_{\text{sample}}$  was the absorbance of a mixture solution of the sample and DPPH. The experiment was repeated three times, each with duplicate samples.

**2.10.2 Superoxide anion radical scavenging activity.** The scavenging activity of superoxide anion radical was detected using the method described by superoxide anion scavenging kit instruction manual-micro method. In brief, a 10  $\mu\text{L}$  Tris-HCl solution (TEMED) and 40  $\mu\text{L}$  ammonium persulfate were added to the control tube and sample tube. 25  $\mu\text{L}$   $\text{H}_2\text{O}$  was only added to the control tube, mixed, and reacted at 25  $^\circ\text{C}$  for 1 min. 25  $\mu\text{L}$  polysaccharide MHHP solution and positive control solution ASA (0.01–0.1  $\text{mg mL}^{-1}$ ) were added to sample tube, and then 50  $\mu\text{L}$  hydroxylamine hydrochloride solution was added to both tubes to reacted at 37  $^\circ\text{C}$  for 30 min. Finally, 50  $\mu\text{L}$  P-aminobenzenesulfonic acid and  $\alpha$ -naphthylamine in acetic acid solutions were mixed into above mixtures and color reactions were conducted at 37  $^\circ\text{C}$  for 20 min. The absorbance was measured at 530 nm. Superoxide radical scavenging activity was calculated according to the following equation:

$$\text{Scavenging activity (\%)} = (1 - A_{\text{sample}}/A_{\text{control}}) \times 100\%$$

**2.10.3 Hydroxyl radical scavenging ability.** Hydroxyl radical ( $^{\bullet}\text{OH}$ ) scavenging activity was measured according to the manual-micro method outlined in the hydroxyl radical scavenging kit instructions. In general, a working solution was prepared beforehand including mixture of phenanthroline-ethanol solution:  $\text{Na}_2\text{HPO}_4 \cdot 12\text{H}_2\text{O}$ - $\text{NaH}_2\text{PO}_4 \cdot 2\text{H}_2\text{O}$  buffer solution:  $\text{FeSO}_4 \cdot 7\text{H}_2\text{O}$  250  $\mu\text{L}$  working solution added to blank tube, control tube, sample tube respectively. After that, 100  $\mu\text{L}$  distilled water to blank tube, 50  $\mu\text{L}$   $\text{H}_2\text{O}_2$  and 50  $\mu\text{L}$  distilled water to control tube and 50  $\mu\text{L}$  4–10  $\text{mg mL}^{-1}$  sample (polysaccharide and positive control) and 50  $\mu\text{L}$   $\text{H}_2\text{O}_2$  to sample tube were mixed and incubated at 37  $^\circ\text{C}$  for 60 min. The absorbance of sample was measured at 536 nm, hydroxyl radical scavenging activity was calculated according to the following equation:

$$\text{Scavenging activity (\%)} = (A_{\text{sample}} - A_{\text{control}}/A_{\text{blank}} - A_{\text{control}}) \times 100\%$$

where  $A_{\text{blank}}$  was the absorbance of the blank (distilled water instead of the sample),  $A_{\text{sample}}$  was the absorbance of the sample, and  $A_{\text{control}}$  was the absorbance of the control (distilled water instead of the  $\text{H}_2\text{O}_2$ ). The experiment was repeated three times, each with duplicate samples.

## 3 Results and discussion

### 3.1 Isolation, purification and molecular weight measurement of the novel polysaccharide

The polysaccharide was obtained *via* the hot water extraction method followed by ethanol precipitation. Among the three different methods used to remove protein impurities in the crude polysaccharide (*i.e.* sewage, trypsin enzyme-sewage combination, trifluoroacetic acid (TFA) methods), the enzyme-

sewage combination method was found to be most suitable to remove proteins from crude MHHP. The enzyme-sewage method is an effective method for removing free protein from polysaccharides, which can be denatured into insoluble matter by centrifugal separation.<sup>38</sup>

After successive separation with DEAE-Sepharose Fast Flow column one fraction denominated MHHP was obtained with yields of respective 1 26.0%. The separation flow diagram for MHHP was presented in Fig. 1, in UV spectrum, there was no obvious absorption at 260 nm and 280 nm, indicating that the nucleic acids and protein impurities were removed from the crude MHHP.

The sugar content of MHHP was determined by the standard curve with anhydrous glucose as a reference. From the standard curve, we calculated the linear regression equation of  $A = 796.2C - 0.3613$  ( $C$  = concentration), with  $r^2 = 0.9945$ , which gave the sugar content of MHHP to be up to 83.13%. The protein content of MHHP was tested with a BCA protein assay kit (Solarbio, China) and the linear regression equation was found to be  $y = 0.9894x + 0.1469$  ( $x$  = BSA protein concentration), with  $r^2 = 0.9908$ , and derived the content of polysaccharide MHHP to be 5%.

The average molecular weight ( $M_w$ ) of MHHP was estimated by using dextrin with different molecular weight as standard. From the standard curve, we calculated the linear regression equation by Empower 2 chromatography workstation software (Fig. 2A), and the  $M_w$  of MHHP was determined to be  $1.61 \times 10^4$  Da with a narrow polydispersity ( $M_w/M_n = 1.33$ ), as seen in Fig. 2C. The GPC results proved that MHHP is a homogeneous polysaccharide with  $M_w = 16.1$  kDa, with  $M_w/M_n = 1.33$ .

### 3.2 Monosaccharide composition and methylation analysis

Monosaccharide composition and ratio in MHHP were confirmed *via* comparing the retention time of monosaccharide obtained from the acetylated derivative of MHHP following acid hydrolysis with that of standard monosaccharides using gas chromatography (GC analysis). Calculation of the peak area (Fig. 3) showed that, the major composition of MHHP was glucose, with possible small portions of galactose and arabinose, which cannot be quantified due to the extremely low content.

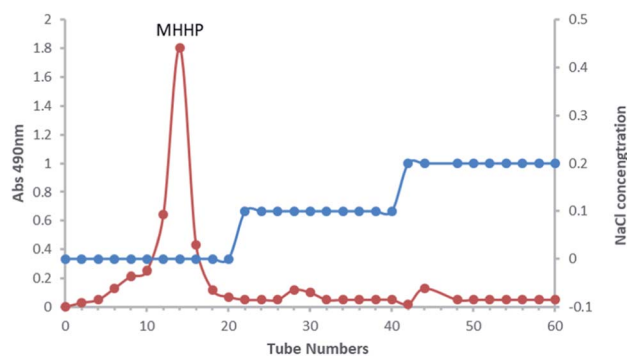


Fig. 1 Elution curve of the water-extractable (MHHP) on a Sepharose Fast Flow column.





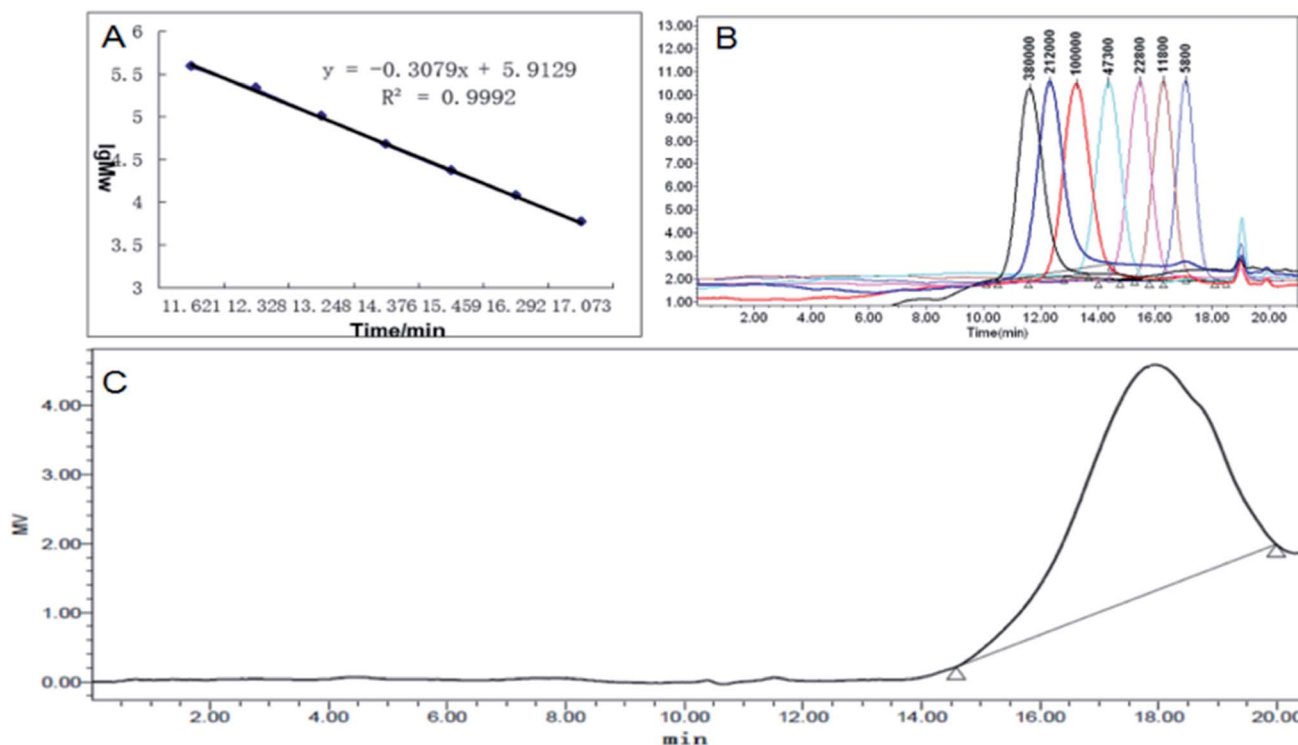


Fig. 2 Determination of molecular weight of MHHP via high-performance gel permeation chromatography. (A) The standard curve of dextrin; (B) GPC profile of dextrin; (C) GPC chromatograph of MHHP polysaccharide.

The glycosidic linkage of monosaccharides in MHHP was identified by automatic reduction of carboxyl groups and subsequent hydrolysis, followed by GC/MS analysis according to a combination of their retention time and mass spectra. As shown in Table 1, the results indicated that three linking types included in MHHP were:  $\rightarrow 4$ -Glc $\alpha$ -(1 $\rightarrow$ ,  $\rightarrow 4,6$ -Glc $\alpha$ -(1 $\rightarrow$  and Glc-(1 $\rightarrow$ .

### 3.3 Characterization of MHHP with UV and FT-IR spectrum

To further characterize MHHP, UV spectroscopy and Fourier-transform infrared (FT-IR) were applied. In UV spectrum (Fig. 4A), there was certain absorbance of protein at 280 nm, which was consistent with protein content determination,

indicating that the removal protein method of MHHP was effective.

The FT-IR spectrum (Fig. 4b) of the MHHP possess the characteristic peaks of polysaccharide (at 3393, 2936, 1742, 1635, and 1416  $\text{cm}^{-1}$ ), where the broad and strong peak of 3393.3  $\text{cm}^{-1}$  is attributed to glycosyl hydroxyl stretching vibration and the weak peak at 2936.5  $\text{cm}^{-1}$  corresponds to C-H asymmetric stretching vibration of methylene group. The free carboxylate group and esterified carboxyl group vibrate at 1635.9  $\text{cm}^{-1}$  and 1742.8  $\text{cm}^{-1}$ . The C=O stretching vibration and the C-H bond peaks in the polysaccharide appeared were observed at 1635.9  $\text{cm}^{-1}$  and 1419.6  $\text{cm}^{-1}$ . The peaks of 1240.0, 1147.6, 1101.4, 1078.2, and 1023.4  $\text{cm}^{-1}$  aroused special interest because the vibration of the ring, the C-O-H stretching

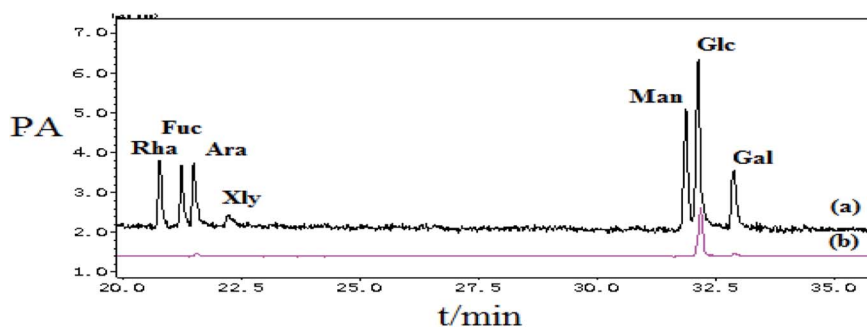


Fig. 3 GC profile of MHHP with acid hydrolysis and acetylation. (a) GC of standard monosaccharides; (b) acid hydrolyzed and acetylated monosaccharides of MHHP polysaccharide.



Table 1 GC-MS analysis of the methylated product of MHHP

Methylated sugar	Mass fragments ( $m/z$ )	Molar ratios	Type of linkage
2,3,4,6-Me <sub>4</sub> -Glc	43, 71, 87, 101, 117, 129, 145, 161, 205	0.125	Glc-(1 →
2,3,6-Me <sub>3</sub> -Glc	43, 87, 99, 101, 113, 117, 129, 131, 161, 173, 233	0.750	→ 4)-Glc-(1 →
2,3-Me <sub>2</sub> -Glc	43, 71, 85, 87, 99, 101, 117, 127, 159, 161, 201	0.125	→ 4,6)-Glc-(1 →

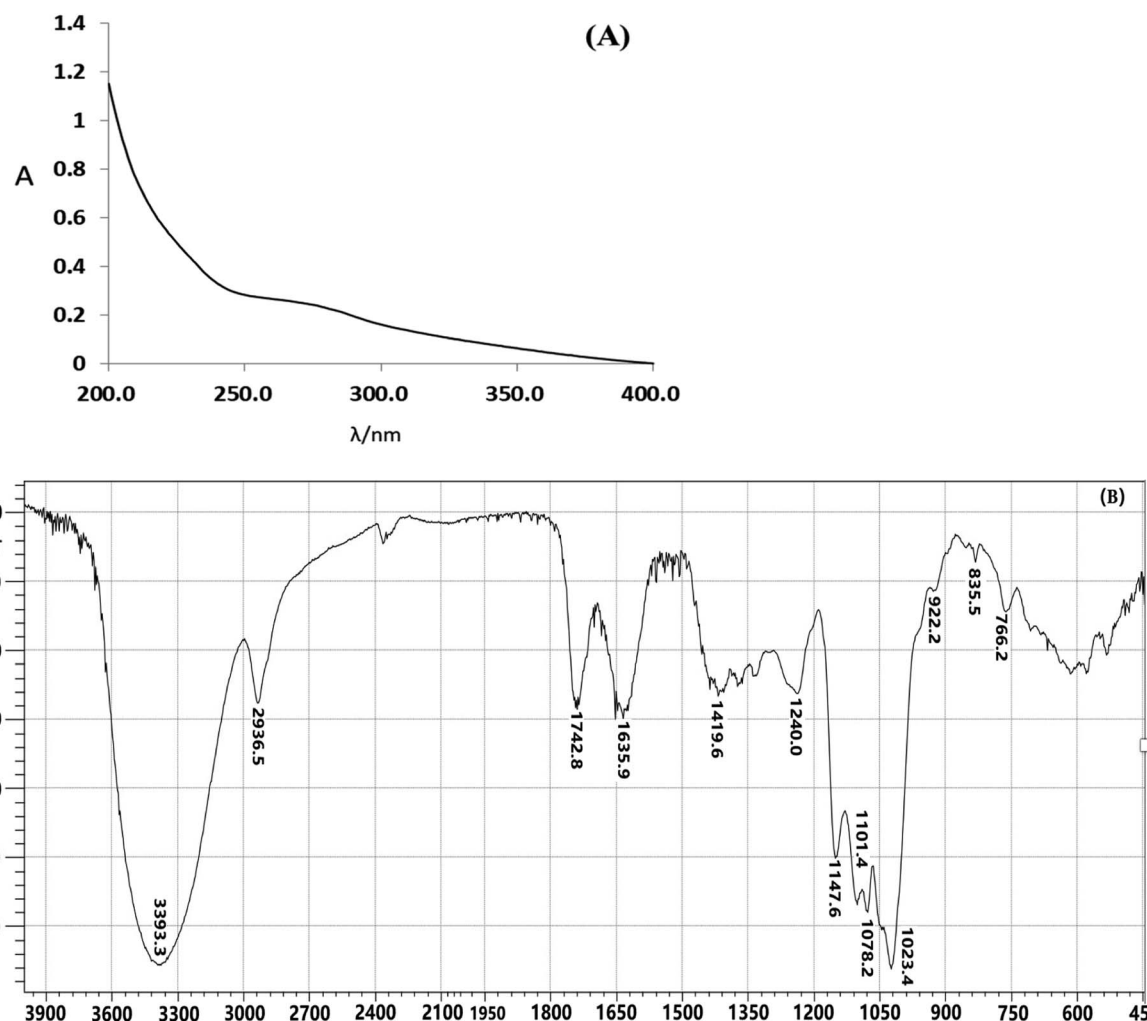


Fig. 4 UV spectrum (A) and Fourier transform infrared (FT-IR) spectrum (B) of MHHP polysaccharide.

vibration and the C–O–C and C–O stretching vibrations of the pyran ring are superimposed in this area. The stretching weak peaks in the regions of 922.2, 835.5, and 766 cm<sup>−1</sup> suggested the

MHHP polysaccharide was an  $\alpha$ -D-glucopyranose derivative.<sup>39</sup> These results indicated that MHHP possessed typical absorption peaks of polysaccharides. The absorption peaks at

Table 2 Chemical shifts of resonance in <sup>13</sup>C and <sup>1</sup>H NMR spectra of MHHP polysaccharide

		Chemical shifts ( $\delta$ , ppm)						
Sugar residues		C1/H1	C2/H2	C3/H3	C4/H4	C5/H5	C6/H6	OCH <sub>3</sub>
A	→ 4)- $\alpha$ -Glc-(1 →	102.4/5.46	74.4/3.73	75.9/4.04	77.2/3.73	73.9/3.93	63.2/3.85	
B	→ 4,6)- $\alpha$ -Glc-(1 →	98.44/5.21	74.2/3.50	75.9/4.04	79.3/3.50	75.6/3.93	70.6/—	
C	T-Glc-(1 →	102.3/5.04	70.6/3.84	72.0/3.95	73.1/4.05	72.6/3.95	62.1/3.73	
D	$\alpha$ -Glc-OMe-(4 →	101.3/4.71	75.5/3.61	75.9/4.04	79.3/3.50	72.6/3.95	62.1/3.73	56.9/3.85

2926  $\text{cm}^{-1}$  and 2866  $\text{cm}^{-1}$  were defined as the characteristic absorption peaks of the ester bond, while MHHP has no absorption peak in the above regions, indicating that there are no protein and ester groups.

### 3.4 NMR analysis of MHHP

$^1\text{H}$  NMR and  $^{13}\text{C}$  NMR analysis of MHHP are listed in Table 2. The corresponding chemical shift between the  $^{13}\text{C}$  NMR and  $^1\text{H}$  NMR spectra were assigned based on the H–H COSY and HSQC spectra results. As shown in Fig. 5, three signals appeared in the anomeric region ( $^1\text{H}$ ) is  $\delta$  5.46, 5.21, and 5.04 ppm, whereas  $^{13}\text{C}$  is in the range of  $\delta$  103–98 ppm in NMR spectra of MHHP. Three cross peaks were spotted in the anomeric regions of the HSQC spectrum, suggesting the existence of three different linkage patterns. Combining the results of linkage analysis with literature,<sup>40,41</sup> the anomeric H signals at  $\delta$  5.46, 5.21, 5.04 and 4.71 ppm (Fig. 5a), and anomeric C signals at  $\delta$  102.4, 102.2, 98.44 and 101.2 ppm (Fig. 5b) were corresponded to H1 and C1 of residue A:  $\rightarrow 4$ - $\alpha$ -GlcP-(1 $\rightarrow$ , residue B:  $\rightarrow 4,6$ - $\alpha$ -GlcP-(1 $\rightarrow$  and residue C: T-GlcP-(1 $\rightarrow$ , and  $\alpha$ -GlcP-OMe-(4 $\rightarrow$  respectively. The  $\delta$  56.9 ppm resonance signal indicates the presence of  $-\text{OCH}_3$  in MHHP.

### 3.5 Scanning electron microscope (SEM)

Fig. 6 exemplified the SEM of natural MHHP polysaccharide at different magnifications to determine the micro-structure image of the polysaccharide. In Fig. 6(A0), the surface morphology of the polysaccharide in dry powder displayed a soft fibrous texture. In Fig. 6(A1), the powdery polysaccharide was clearly observed to contain fibrous filaments and spherical particles at 5k magnification. When the sample was magnified to 20k and 80k, the polysaccharide was visible as a thin layer about 40–50 nm with a smooth and near surface. Fig. 6(B0–B3) are SEM images of the polysaccharide scattered in ethanol by ultrasound. It is a flexible, thin lamellar structure and spherical particles have disappeared as seen in Fig. 6(B1) at 5k magnification. When sample was magnified to 20k and 150k, the polysaccharide also appeared as a thin layer about 40 nm thick with smooth and near surface.

### 3.6 Immunomodulatory activity of MHHP

**3.6.1 Effect of MHHP on spleen cell proliferation.** In the process of cellular and humoral immunity, T and B lymphocytes are important effector cells involved in the body's immune response. Under the stimulation of mitogens ConA and LPS, lymphocytes can be into division and proliferation, where ConA is the stimulator of T lymphocyte proliferation, and LPS is the stimulator of B lymphocyte proliferation. During the development of the body's immune response, T lymphocytes are mainly involved in cellular immune responses, and B lymphocytes are mainly involved in humoral immune responses. Therefore, the transformation reaction and the degree of proliferation of lymphocyte have become effective indicators for measuring the immune function of the body.<sup>42</sup>

To examine whether MHHP polysaccharide was able to activate the functional proliferation of spleen lymphocytes, the

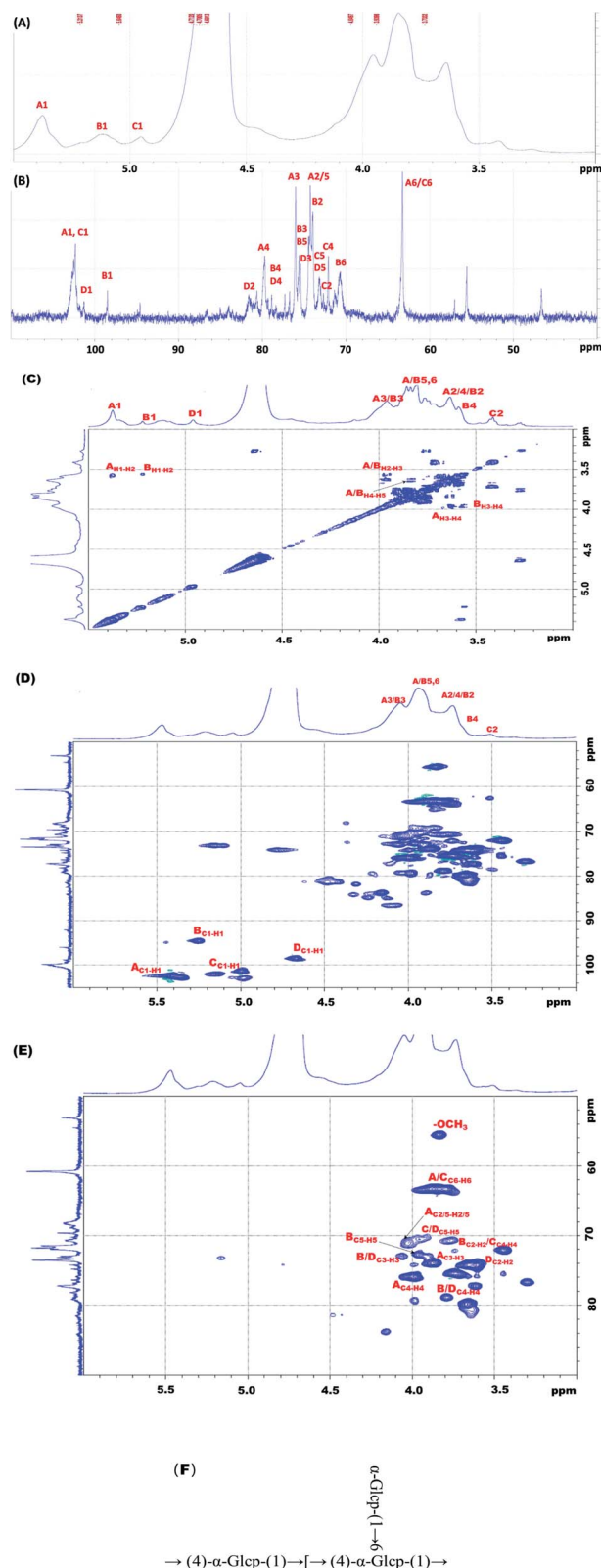


Fig. 5 Analysis of structure of MHHP by NMR. (A)  $^1\text{H}$  NMR spectrum; (B)  $^{13}\text{C}$  NMR spectrum; (C) COSY spectrum; (D)–(E) HSQC spectrum; (F) determined structure of MHHP polysaccharide. Solvent for NMR:  $\text{D}_2\text{O}$ . Temperature: 40  $^\circ\text{C}$ .

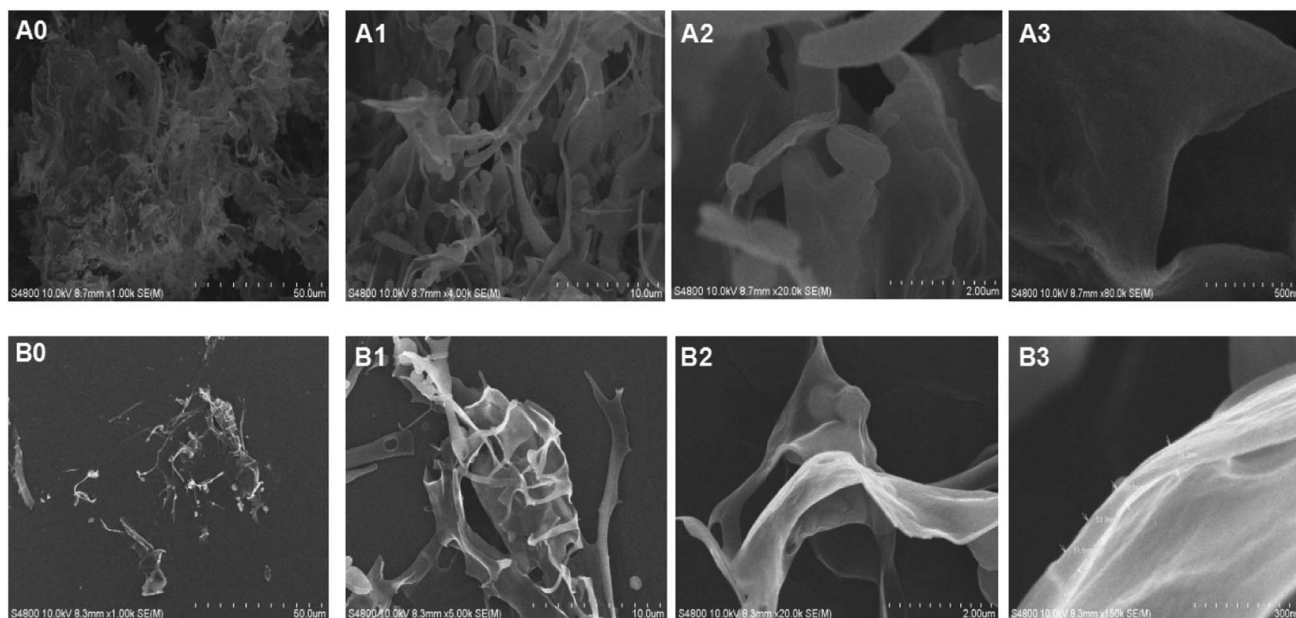


Fig. 6 Digital SEM photographs of MHHP polysaccharide in freeze-dry powder (A0–A3) and in ethanol (B0–B3) detected at magnifications of 1k, 5k, 20k and 80k, respectively.

mouse spleen cells were incubated with 5, 40 and 200  $\mu\text{g mL}^{-1}$  of MHHP polysaccharide for 48 h. As depicted in Fig. 7a, compared to the untreated cell control group and LPS positive control group, there were obvious proliferation activities as the concentration of MHHP increased, indicating that MHHP have significant stimulatory effects on spleen lymphocytes in a dose-dependence manner at concentrations of 5–200  $\mu\text{g mL}^{-1}$ .

**3.6.2 Effect of MHHP on IFN- $\gamma$  and IL-2 secretion.** Cytokines released by lymphocytes are crucial information molecules in immune regulation. Among them, IL-2 is essential for the proliferation of T cells, and other cytokines are involved in the differentiation of T cells. In order to further illustrate the immune-stimulatory activity of MHHP, IFN- $\gamma$  and IL-2 levels in the supernatant of cells treated with different concentrations of MHHP *in vitro* were measured by ELISA. As shown in Fig. 7b, in the concentration range of 5–200  $\mu\text{g mL}^{-1}$ , the secretion of IFN- $\gamma$  in the MHHP treatment group significantly increased ( $p < 0.01$ ) in a dose-dependent manner comparing to that of the cell control group. However, the production of interleukin-2 (IL-2) in the MHHP groups slightly increased compared with cell control for 48 h. Moreover, there was no significant difference in expression levels of IL-2 between the three MHHP treatment groups and cell control groups ( $p > 0.05$ ) (see Fig. 7c).

**3.6.3 Activation effect of MHHP on macrophage *in vitro*.** In the immune system, the stimulation of immune cells such as lymphocytes, macrophages and dendritic cells play an essential role in promoting immunity.<sup>43</sup> Polysaccharides isolated from Traditional Chinese Medicine have been shown to motivate innate and cellular immunity through interaction with immune cells, regulate immune signals in an appropriate manner, and promote the body's immune system to resist certain bacterial or viral infections. Studies have shown that plant polysaccharides have close connections to immune regulation. When immune

cells are activated, these responses then activate the key transcription factor nuclear factor- $\kappa\text{B}$  (NF- $\kappa\text{B}$ ) or mitogen-activated protein kinase (MAPK) signaling pathways, thereby inducing inflammatory factors such as IL-2, TNF- $\alpha$  and IL-6 expression, and gene transcription in immune cells.

The potential immune-modulatory activity of MHHP was examined using a mouse macrophage cell line, RAW 264.7 cell to demonstrate the increase or decrease in the concentration of TNF- $\alpha$ , IL-6, IL-1 $\beta$  and NO. As illustrated in Fig. 8, stimulatory activity of MHHP on macrophage was demonstrated by dose-dependent increase in TNF- $\alpha$  (Fig. 8a), IL-6 (Fig. 8b) and NO (Fig. 8c) secretion by RAW 267.4 cells cultured with MHHP for 48 h.

The expression levels of Tumor Necrosis Factor (TNF- $\alpha$ ) were significantly elevated in the LPS and MHHP treatment groups ( $p < 0.01$ ) compared to the cell control (Fig. 8a). Meanwhile, significant increases of the secretion levels of interleukin-6 (IL-6) and NO production were observed in LPS ( $p < 0.05$ ) and high-dose treatment groups ( $p < 0.01$ ) (Fig. 8b and c). Those results proved that MHHP activates immune function by inducing macrophages to secrete the related cytokines.

### 3.7 Antioxidant activities of MHHP

The antioxidant activity of MHHP was evaluated by three different chemical model methods, including 2, 2-diphenyl-1-picrylhydrazyl (DPPH), hydroxyl and superoxide anion radical scavenging ability assay *in vitro*. The results confirmed that MHHP can scavenge hydroxyl, DPPH and superoxide anion radicals in a certain degree, as shown in Fig. 9.

The DPPH radical has a single electron and a strong absorption at 517 nm due to the purple visible in alcohol solution. Antioxidants (or free radical scavengers) can pair



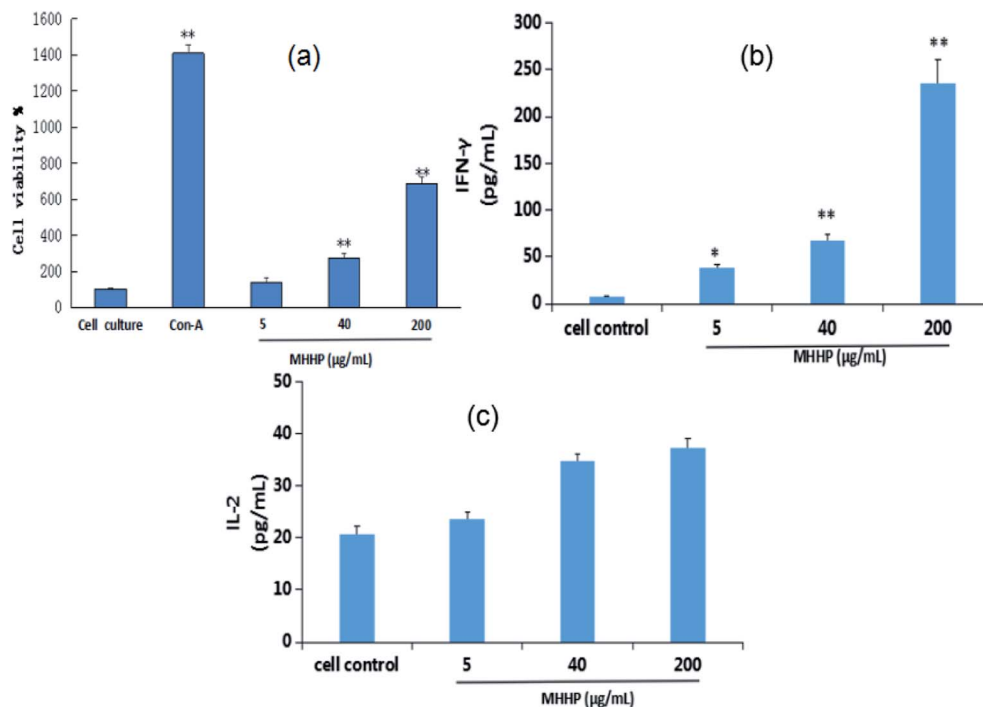


Fig. 7 Effect of MHHP on lymphocyte proliferation *in vitro* (A), on IFN- $\gamma$  (B) and IL-2 (C) secretion by mouse spleen lymphocyte ( $x \pm \text{SD}$ ,  $n = 3$ ), Con-A was used as a positive control. The mouse lymphocyte cells were cultured in the presence of MHHP at three different concentrations for 48 h. The culture supernatant collected were assayed the levels of IFN- $\gamma$ . \* $p < 0.05$ , \*\* $p < 0.01$  versus cell control.

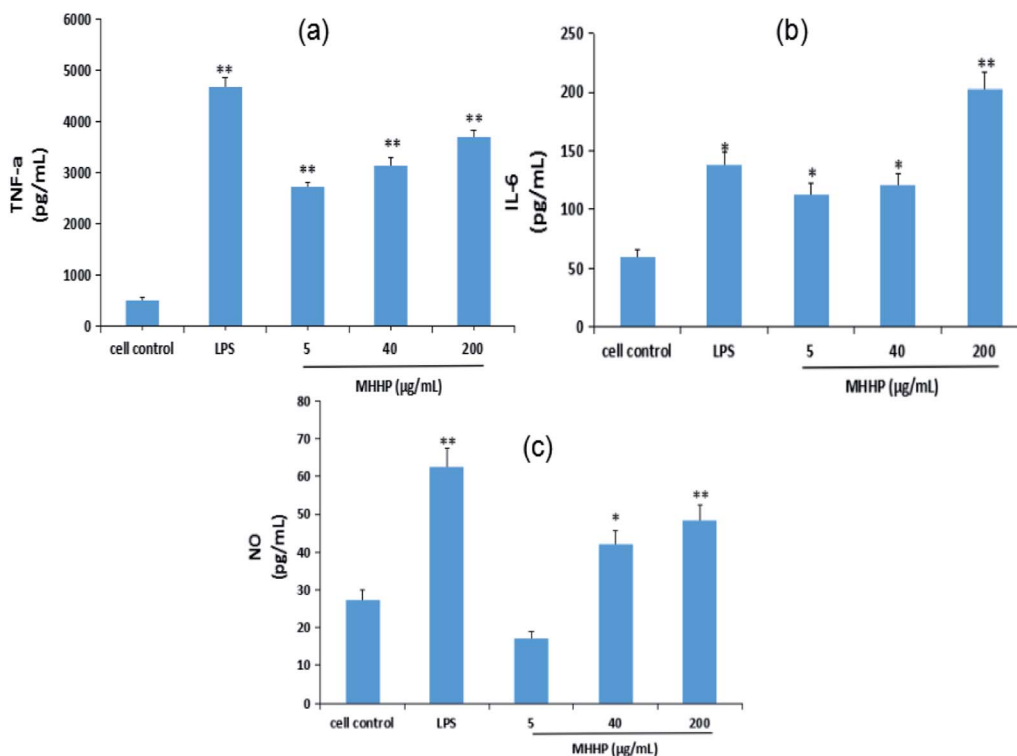


Fig. 8 Immunomodulatory activity of MHHP polysaccharide on RAW 264.7 cell. RAW 264.7 cells were cultured in the presence of MHHP at the three different concentrations for 48 h. The culture supernatant collected were assayed for the levels of TNF- $\alpha$  (a), IL-6 (b), and NO contents (c). LPS was used as a positive control, \* $p < 0.05$ , \*\* $p < 0.01$  versus cell control.



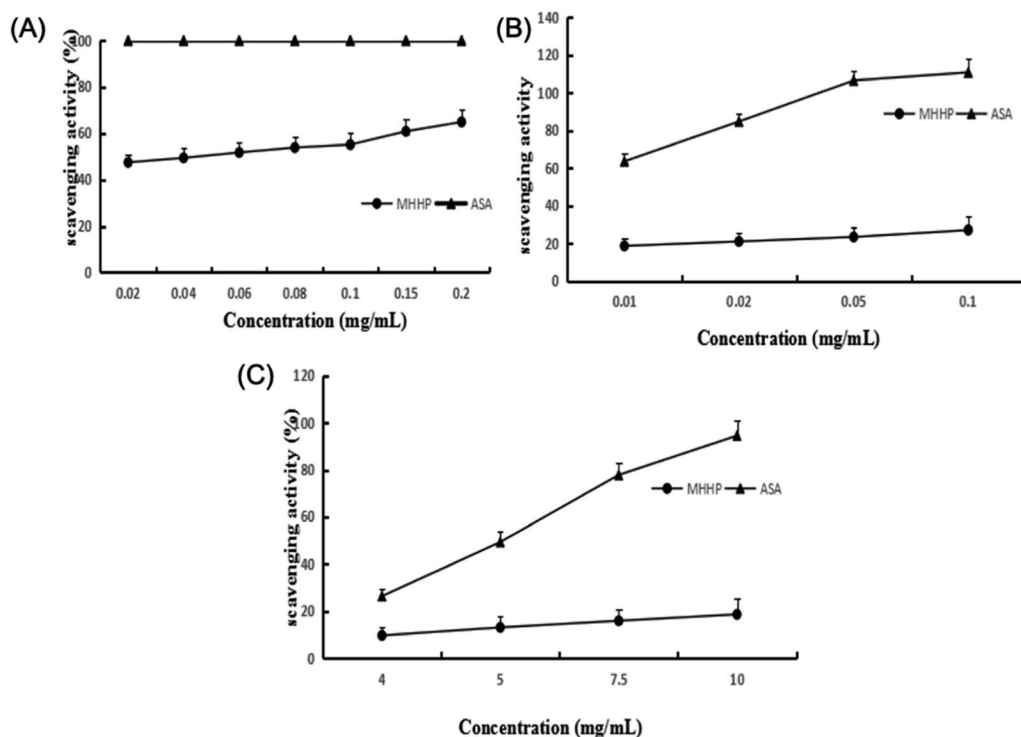


Fig. 9 Antioxidant activity assay of MHHP. (A) DPPH radical scavenging assay; (B) superoxide anion-scavenging activity assay; (C) hydroxyl radical scavenging ability assay; values are means  $\pm$  SD,  $n = 3$ .

single electrons, thereby reducing the  $A_{517\text{nm}}$  value and discoloring the solution. Because of this change, the quantity of electrons accepted becomes quantitative with polysaccharides, so scavenging DPPH free radicals and antioxidant capacity can be measured with a UV-Vis spectrophotometer. As shown in Fig. 9a, the scavenging activities of MHHP inhibited DPPH radicals proportionally to concentration in ranges from 0.02 to 0.2 mg mL<sup>-1</sup> (47.47–64.93%). Compared to the ASA group, MHHP showed lower DPPH scavenging activity.

Superoxide anion free radicals are a kind of free radical produced during the metabolism of organisms, which can attack biological macromolecules such as lipids, proteins, nucleic acids and polyunsaturated fatty acids, etc. This causes them to cross-link or break, causing the damage of cell structure and function, which is closely related to the body's aging and pathological changes. Research on scavenging superoxide anion free radicals has received extensive attention.<sup>44</sup> The AP-TEMED system produces superoxide anions and reacts with hydroxylamine hydrochloride to form NO<sup>2-</sup>. The action of NO<sup>2-</sup> with *p*-aminobenzenesulfonic acid and  $\alpha$ -naphthylamine produces a red compound with a characteristic absorption peak at 530 nm. The scavenging capacity of oxygen anions is inversely related to the absorbance at 530 nm. As shown in Fig. 9b, the scavenging potencies of MHHP against superoxide anion free radicals showed dose-dependent mode from 0.01 to 0.1 mg mL<sup>-1</sup> (18.83–27.24%). ASA, which was performed as a positive control, exhibited more potent superoxide anion free radicals scavenging effects than the MHHP polysaccharide.

H<sub>2</sub>O<sub>2</sub>/Fe<sup>2+</sup> generates hydroxyl radicals through the Fenton reaction, Fe<sup>2+</sup> in the phenanthroline-Fe<sup>2+</sup> aqueous solution oxidized into Fe<sup>3+</sup>, resulting in decreasing absorbance at 536 nm. The degree of decreasing rate in absorbance at 536 nm reflects the sample's ability to scavenge hydroxyl radicals. As shown in Fig. 9c, the scavenging ability of MHHP against hydroxyl free radical reached maximum value of 18.63% at 10 mg mL<sup>-1</sup>. ASA, a positive control, showed higher hydroxyl radical scavenging effect compared with the MHHP polysaccharide. It turns out that the polysaccharide extracted from *Mirabilis himalaica* has certain antioxidant activity. However, the detection of these antioxidant activities is only established in chemical systems *in vitro*. Therefore, animal or cell experiments *in vivo* are needed to further verify the reliability of its antioxidant activity.

## 4. Conclusion

In this study, an acidic homogeneous polysaccharide MHHP, acquired from *Mirabilis himalaica*, exhibited the primary structure which consisted of  $\alpha$ -D-glucan containing (1→4)-linked residues. MHHP could induce the secretion of cytokine (IL-2, INF- $\gamma$ , IL-6, TNF- $\alpha$ ) in spleen lymphocytes and macrophages *in vitro*. Therefore, MHHP polysaccharide may potentially enhance the macrophage related innate immune response. MHHP also displayed moderate antioxidant activity compared with those of ASA by three radical scavenging assay. In summary, the current investigation enriched the exploration of polysaccharides from *Mirabilis himalaica*, the therapeutic

application of which needs to be further explored specifically with respect to its structure–activity relationship and efficacy in animal models. In addition,  $\alpha$ -(1→4)-glucan from *Radix Aconiti Lateralis Preparata* (Fuzi) and *Sophora subprosrate* all were reported for their immune-modulating effects, while the structural characterizations from each other were slightly different especially in branch.<sup>45,46</sup> The relationship between the various pharmacological functions and structure need to be further explored and studied.

## Live subject statement

“All animal procedures were performed in accordance with the Guidelines for Care and Use of Laboratory Animals of “Inner Mongolia Medical” University and experiments were approved by the Animal Ethics Committee of “Inner Mongolia Medical University”.

## Author contributions

Surina Bo: conceptualization, methodology, investigation, writing – original draft, project administration, funding acquisition. Wenjie Han, Mu Dan, Liang bao: formal analysis, data curation, validation, writing – review & editing. Sarangua Ochir, Tegshi Muschin, Huricha Baigude: conceptualization, writing – review & editing, investigation, visualization.

## Conflicts of interest

The authors declare no conflict of interest.

## Acknowledgements

This work was supported in part by the National Natural science Foundation of China (22167019), the Natural science Fund of Inner Mongolia Province, China (2019LH02002), and the Natural science fund of Inner Mongolia Medical University, China (YKD2018KJBW003).

## References

- 1 L. Q. Li, H. Quan, L. S. Wang, C. P. Cai and X. Z. Lan, The nutritional organ yield and boeravinone C spatial dynamics of *Mirabilis himalaica*, *Jiangsu Agric. Sci.*, 2014, **42**(7), 255–258.
- 2 Qinghai Institute for Tibetan Medicines, *Tibetan Drugs in China [M]*, Shanghai Scientific and Technical Publishers, Shanghai, 1996.
- 3 State Administration of Chinese Medicine, *Chinese Materia Medica, Tibetan Drugs Edition [M]*, Shanghai Science and Technology Publishing House, Shanghai, 2002.
- 4 A. Dubreuil, *Divine Farmer's Classic of Material Medica*, Foreign language press, Beijing, 2015.
- 5 C. P. Cai, S. L. Wang, H. Quan, J. Luo, F. C. Guan and X. Z. Lan, On Morphological Diversity in Germplasm Resources of Tibetan Herbal Medicine *Mirabilis Himalaica*, *J. Southwest China Norm. Univ., Nat. Sci. Ed.*, 2013, **38**(12), 61–66.
- 6 X. Z. Lan, H. Quan, L. Q. Li, X. L. Xia and W. L. Yin, Study on the germination properties and quality of seeds of *Mirabilis himalaica*, *Seed*, 2014, **33**(9), 6–10.
- 7 G. L. Zhang, Q. Y. Xing and M. Z. Zhang, Glycolipids from *Mirabilis himalaica*, *Phytochemistry*, 1997, **45**, 1213–1215.
- 8 G. L. Zhang, Z. Z. Zhou and B. G. Li, Mirabliamide: a new feruoyl amide from mirablis himalaica, *Nat. Prod. Res. Dev.*, 1998, **10**, 12–14.
- 9 S. Y. Zhou, G. W. Wang, Y. L. Zou, L. Q. Deng, M. X. Liu, Z. H. Liao, X. Z. Lan and M. Chen, A new diphenyl ether derivative from *Mirabilis himalaica*, *Nat. Prod. Res.*, 2017, **31**(9), 1034.
- 10 L. H. Lang, H. X. Fang, Y. J. Hu, Y. L. Zou, P. P. Yang, X. Z. Lan, Z. H. Liao and M. Chen, Mirabijalone E.: A novel rotenoid from *Mirabilis himalaica* inhibited A549 cell growth in vitro and in vivo, *J. Ethnopharmacol.*, 2014, **155**(1), 326–333.
- 11 N. Sharon, Carbohydrates as future anti-adhesion drugs for infectious diseases, *Biochim. Biophys. Acta, Gen. Subj.*, 2006, **1760**(4), 527–537.
- 12 C. L. Zhao, G. Wang, C. B. Liu, Y. Jin and Z. Xing, Structural characterization and antiviral activity of a novel heteropolysaccharide isolated from *grifola frondosa* against enterovirus 71, *Carbohydr. Polym.*, 2016, **144**, 382–389.
- 13 C. J. Li, Y. Z. Zhang and W. F. Meng, The hypoglycemic mechanism of *Angelica polysaccharide* in type-2 diabetic rats, *Journal of Qiqihar Medical College*, 2007, **28**, 1422–1424.
- 14 C. X. Yang, Y. Gou, J. Chen, J. An, W. X. Chen and F. D. Hu, Structural characterization and antitumor activity of a pectic polysaccharide from *Codonopsis pilosula*, *Carbohydr. Polym.*, 2013, **98**(1), 886–895.
- 15 T. T. Long, Z. J. Liu, J. C. Shang, X. Zhou, S. Yu, H. Tian and Y. X. Bao, Polygonatum sibiricum, polysaccharides play anti-cancer effect through TLR4-MAPK/NF- $\kappa$ B signaling pathways, *Int. J. Biol. Macromol.*, 2018, **111**, 813–821.
- 16 L. Chen, R. Long, G. Huang and H. Huang, Extraction and antioxidant activities in vivo of pumpkin polysaccharide, *Ind. Crops Prod.*, 2020, **146**, 112199.
- 17 F. Chen, G. L. Huang and H. L. Huang, Preparation, analysis, antioxidant activities in vivo of phosphorylated polysaccharide from *momordica charantia*, *Carbohydr. Polym.*, 2020, **252**, 117179.
- 18 B. X. Du, Y. P. Fu, X. Wang, H. Q. Jiang, Q. T. Lv, R. K. Du, Y. Yang and R. Rong, Isolation, purification, structural analysis and biological activities of water-soluble polysaccharide from *Glehniae radix*, *Int. J. Biol. Macromol.*, 2019, **128**, 724–731.
- 19 G. Hou, X. Chen, J. Li, Z. Ye, S. Zong and M. Ye, Physicochemical properties, immunostimulatory activity of the lachnum polysaccharide and polysaccharide-dipeptide conjugates, *Carbohydr. Polym.*, 2019, **206**, 446–454.
- 20 J. Tang, H. Zhen, N. Wang, Q. Yan, H. Jing and Z. Jiang, Curdlan oligosaccharides having higher immunostimulatory activity than curdlan in mice treated



- with cyclophosphamide, *Carbohydr. Polym.*, 2019, **207**, 131–142.
- 21 J. Huo, Y. Lu, Y. Jiao and D. Chen, Structural characterization and anticomplement activity of an acidic polysaccharide from *hedyotis diffusa*, *Int. J. Biol. Macromol.*, 2020, **155**, 1553–1560.
- 22 X. Zhang, N. Zhang, J. Kan, R. Sun, S. Tang and Z. Wang, Anti-inflammatory activity of alkali-soluble polysaccharides from *arctium lappa* L. and its effect on gut microbiota of mice with inflammation, *Int. J. Biol. Macromol.*, 2020, **154**, 773–787.
- 23 S. Tuvaanjav, S. Q. Han, K. Masashi, C. J. Ma, T. Kanamoto, H. Nakashima and T. Yoshida, Isolation and antiviral activity of water-soluble *Cynomorium songaricum* Rupr. polysaccharides, *J. Asian Nat. Prod. Res.*, 2016, **18**(2), 159–171.
- 24 M. L. Jin, K. Zhao, Q. S. Huang and P. Shang, Structural features and biological activities of the polysaccharides from *Astragalus membranaceus*, *Int. J. Biol. Macromol.*, 2014, **64**, 257–266.
- 25 X. B. Yang, Y. Zhao, H. F. Wang and Q. B. Mei, Macrophage activation by an acidic polysaccharide isolated from *Angelica sinensis* (Oliv.) Diels, *J. Biochem. Mol. Biol.*, 2007, **40**, 636–643.
- 26 Y. S. Cui, Y. X. Li, S. L. Jiang, Z. Fu and W. Qiao, Isolation, purification, and structural characterization of polysaccharides from *atractylodis macrocephalae* rhizoma and their immunostimulatory activity in raw264.7 cells, *Int. J. Biol. Macromol.*, 2020, **163**, 270–278.
- 27 K. Zhou, H. Taoerdahong, J. Bai, A. Bakasi and C. Dong, Structural characterization and immunostimulatory activity of polysaccharides from *pyrus sinkiangensis* yu, *Int. J. Biol. Macromol.*, 2020, **157**, 444–451.
- 28 C. O. Pandeirada, L. Maricato, S. F. Sónia, V. G. Correia, B. A. Pinheiro, D. V. Evtuguin, A. S. Palma, A. Correia, M. Vilanovad, M. A. Coimbra and N. Cláudia, Structural analysis and potential immunostimulatory activity of *nannochloropsis oculata* polysaccharides, *Carbohydr. Polym.*, 2019, **222**, 114962.
- 29 M. J. Elder, S. J. Webster, R. L. Chee, D. Williams, J. S. Hill Gaston and C. J. Goodall,  $\beta$ -Glucan size controls Dectin-1-mediated immune responses in human dendritic cells by regulating IL-1 $\beta$  production, *Front. Immunol.*, 2017, **8**, 791–802.
- 30 S. B. Han, Y. D. Yoon, H. J. Ahn, H. S. Lee, C. W. Lee, W. K. Yoon, S. K. Park and H. M. Kim, Toll-like receptor-mediated activation of B cells and macrophages by polysaccharide isolated from cell culture of *acanthopanax senticosus*, *Int. Immunopharmacol.*, 2003, **3**(9), 1301–1312.
- 31 S. Shukla, V. K. Bajpai and M. Kim, Plants as potential sources of natural immunomodulators, *Rev. Environ. Sci. Bio/Technol.*, 2014, **13**(1), 17–33.
- 32 J. Wang, S. Li and Y. Fan, Anti-fatigue activity of the water-soluble polysaccharides isolated from *Panax ginseng* C. A. Meyer, *J. Ethnopharmacol.*, 2010, **130**(2), 420–423.
- 33 B. Yuan, J. N. Han, Y. L. Cheng, S. J. Cheng, D. C. Huang, J. M. David and C. J. Cao, Identification and characterization of antioxidant and immune-stimulatory polysaccharides in flaxseed hull, *Food Chem.*, 2020, **315**, 126266.
- 34 S. Bo, D. Mu, W. X. Li and P. Zhang, Characterizations and Immunostimulatory Activities of a Polysaccharide from *Arnebia euchroma* (Royle) Johnst. Roots, *Int. J. Biol. Macromol.*, 2019, **125**, 791–799.
- 35 R. L. Taylor and H. E. Conrad, Stoichiometric depolymerization of polyuronides and glycosaminoglycuronans to monosaccharides following reduction of their carbodiimide-activated carboxyl groups, *Biochemistry*, 1972, **11**(8), 1383–1388.
- 36 I. M. Sims, S. M. Carnachan, T. J. Bell and S. F. R. Hinkley, Methylation analysis of polysaccharides: technical advice, *Carbohydr. Polym.*, 2018, **188**, 1–7.
- 37 J. H. Xie, Z. J. Wang, M. Y. Shen, S. P. Nie, B. Gong, H. S. Li, Q. Zhao, W. J. Li and M. Y. Xie, Sulfated modification, characterization and antioxidant activities of polysaccharide from *Cyclocarya paliurus*, *Food Hydrocolloids*, 2016, **53**, 7–15.
- 38 J. C. Chen, S. Tian, X. Y. Shu, H. T. Du, N. Li and J. R. Wang, Extraction, characterization and immunological activity of polysaccharides from *rhizoma gastrodiae*, *Int. J. Mol. Sci.*, 2016, **17**(7), 1011–1025.
- 39 J. L. Chen, W. S. Pang, W. T. Shi, B. Yang, Y. J. Kan, Z. D. He and J. Hu, Structural Elucidation of a Novel Polysaccharide from *Pseudostellaria heterophylla* and Stimulating Glucose Uptake in Cells and Distributing in Rats by Oral, *Molecules*, 2016, **21**(9), 1233.
- 40 A. X. Luo, Z. F. Ge, Y. J. Fan, A. S. Luo, Z. Chun and X. J. He, In Vitro and In Vivo Antioxidant Activity of a Water-Soluble Polysaccharide from *Dendrobium denneanum*, *Molecules*, 2011, **16**(2), 1579–1592.
- 41 C. Teng, P. Qin, Z. Shi, W. Zhang and G. Ren, Structural characterization and antioxidant activity of alkali-extracted polysaccharides from quinoa, *Food Hydrocolloids*, 2020, **113**, 106392.
- 42 L. Ren, J. Zhang and T. Zhang, Immunomodulatory activities of polysaccharides from *ganoderma* on immune effector cells, *Food Chem.*, 2020, **340**, 127933.
- 43 Y. Yue, M. Shen, Q. Song and J. Xie, Biological activities and pharmaceutical applications of polysaccharide from natural resources: a review, *Carbohydr. Polym.*, 2018, **183**, 91–101.
- 44 A. Q. Zhang, X. Q. Li, C. Xing, J. H. Yang and P. L. Sun, Antioxidant activity of polysaccharide extracted from *Pleurotus eryngii* using response surface methodology, *Int. J. Biol. Macromol.*, 2014, **65**(5), 28–32.
- 45 X. Yang, Y. Wu, C. Zhang, S. Fu, J. Zhang and C. Fu, Extraction, Structural characterization, and immunoregulatory effect of a polysaccharide fraction from *radix aconiti lateralis preparata* (fuzi), *Int. J. Biol. Macromol.*, 2020, **143**, 314–324.
- 46 X. H. Shuai, T. J. Hu, H. L. Liu, Z. J. Su, Z. Yun and Y. H. Li, Immunomodulatory effect of a *sophora subprostrate* polysaccharide in mice, *Int. J. Biol. Macromol.*, 2010, **46**(1), 79–84.